Insect Biochemistry and Molecular Biology 109 (2019) 43–51

Contents lists available at ScienceDirect

Insect Biochemistry and Molecular Biology

journal homepage: www.elsevier.com/locate/ibmb

Maelstrom regulates spermatogenesis of the silkworm, *Bombyx mori*

Kai Chen[a,b], Shuqing Chen[a,b], Jun Xu[a], Ye Yu[a,b], Zulian Liu[a], Anjiang Tan[a], Yongping Huang[a,*]

[a] Key Laboratory of Insect Developmental and Evolutionary Biology, Institute of Plant Physiology and Ecology, Shanghai Institutes for Biological Sciences, Chinese Academy of Sciences, Shanghai, 200032, China
[b] University of Chinese Academy of Sciences, Beijing, 100049, China

ARTICLE INFO

Keywords:
Spermatogenesis
Maelstrom
CRISPR/Cas9
Bombyx mori

ABSTRACT

The spermatogenesis of animal is essential for the reproduction and a very large number of genes participate in this procession. The *Maelstrom* (*Mael*) is identified essential for spermatogenesis in both *Drosophila* and mouse, though the mechanisms appear to differ. It was initially found that *Mael* gene is necessary for axis specification of oocytes in *Drosophila*, and recent studies suggested that *Mael* participates in the piRNA pathway. In this study, we obtained *Bombyx mori Mael* mutants by using a binary transgenic CRISPR/Cas9 system and analyzed the function of *Mael* in *B. mori*, a model lepidopteran insect. The results showed that *BmMael* is not necessary for piRNA pathway in the ovary of silkworm, whereas it might be essential for transposon elements (TEs) repression in testis. The *BmMael* mutation resulted in male sterility, and further analysis established that *BmMael* was essential for spermatogenesis. The spermatogenesis defects occurred in the elongation stage and resulted in nuclei concentration arrest. RNA-seq and qRT-PCR analyses demonstrated that spermatogenesis defects were associated with tight junctions and apoptosis. We also found that *BmMael* was not involved in the silkworm sex determination pathway. Our data provide insights into the biological function of *BmMael* in male spermatogenesis and might be useful for developing novel methods to control lepidopteron pests.

1. Introduction

Spermatogenesis was vital for propagation (Agarwal and Said, 2003; Martin, 2008). The molecular mechanisms of spermatogenesis differ, although the development stages of spermatogenesis are similar across species. The process of spermatogenesis could be generally divided into three stages: the spermatogonial stage, during which germ cells undergo mitosis; the spermatocyte stage, during which germ cells undergo meiosis; and the spermatid stage, during which germ cells complete morphogenetic changes necessary to form mature spermatozoa (Kanippayoor et al., 2013; Fairchild et al., 2017; Siddall and Hime, 2017).

In *Drosophila*, which is a model system for many processes such as stem cell development and cytoskeleton modification (Soper et al., 2008; Fairchild et al., 2017), the spermatogonial stage, occured at the apical end of the testis. During this stage, one germline stem cell asymmetrically divided into two different cells: a new stem cell and a primary spermatogonium, which was also known as gonialblast (Kanippayoor et al., 2013; Siddall and Hime, 2017). This was followed by four cycles of mitosis, such that one gonialblast produces sixteen primary spermatocytes. Subsequently, the germ cells enter into the spermatocyte stage, during which they give rise to sixty-four round spermatids through a meiosis program. Finally, during the spermatid stage, nuclei are remodeled and elongated, and mature spermatozoa are generated. Upon completion of spermatogenesis, the germ cells move from the apical end to distal end of testis (Matunis et al., 2012; Rettie and Dorus, 2012; Fairchild et al., 2015, 2017).

Bombyx mori, the model lepidopteran insect, has dimorphic sperm: eupyrene sperm (nucleated) and apyrene sperm (anucleated) (Osanai et al., 1987; Cook and Wedell, 1999). Like the sperm cells of other insects, the mature eupyrene sperm of *B. mori* has two main parts: an elongated head containing the nucleus and a long tail. In *B. mori*, 256 eupyrene sperm form a bundle that is enveloped by cyst cells. Apyrene sperm are shorter than the eupyrene sperm, and nuclei of diverse sizes are located in the middle region of the apyrene sperm (Osanai et al., 1987; Kawamura et al., 1998; Yamashiki and Kawamura, 2003). The eupyrene sperm fertilize eggs, while Eupyrene sperm play a vital role in assisting fertilization; however, their exact function is still controversial (Riemann and George, 1973; Osanai et al., 1987; Sahara and Takemura, 2003). Thus, despite a long history of study of silkworm sperm (Meves, 1902), the mechanism of spermatogenesis in the silkworm is still unclear.

Maelstrom (*Mael*) was initially investigated in *Drosophila*, in which it plays a vital role in axis specification in oocytes (Clegg et al., 1997). The

* Corresponding author.
E-mail address: yphuang@sibs.ac.cn (Y. Huang).

https://doi.org/10.1016/j.ibmb.2019.03.012
Received 19 November 2018; Received in revised form 3 March 2019; Accepted 28 March 2019
Available online 07 April 2019
0965-1748/

MAEL protein has two characterized domains: It has a High Mobility Group (HMG) box at N terminus and a unique MAEL domain in the central region (Soper et al., 2008; Matsumoto et al., 2015; Sato and Siomi, 2016). Subsequent studies showed *Mael* is essential for spermatogenesis in *Drosophila* and mouse, and studies in recent years proved *Mael* also participates in the piRNA pathway (Soper et al., 2008; Pek et al., 2009; Sienski et al., 2012).

In animals, the large numbers of transposon elements (TEs) pose a serious threat to genome stability. The consequences of genomic damage are particularly serious in germ cells. Through silencing of TEs, the piRNA pathway acts as a guardian of the genome in germ cells (Slotkin and Martienssen, 2007; Siomi et al., 2011; Czech and Hannon, 2016; Tóth et al., 2016). Previous studies showed that *Mael* is essential for silencing of TEs but not for biogenesis of piRNA in *Drosophila* (Sienski et al., 2012). In *B. mori*, a PIWI-interacting RNA (piRNA) produced from the piRNA precursor named *Fem* was shown to be involved in sex determination, and deletion of the piRNA factor *piwi* results in partial sexual reversal (Kiuchi et al., 2014; Li et al., 2018). The *B. mori* MAEL domain functions as a RNA-binding module (Chen et al., 2015). However, the biological function of *Mael* is unexplored in *B. mori*.

In the present study, we obtained *BmMael* mutants using a binary transgenic CRISPR/Cas9 system and performed functional analyses in the silkworm. We found that *BmMael* is not required for sex determination in the silkworm, but it was essential for spermatogenesis. Our data showed that mutation of *BmMael* induces spermatogenesis defects that occurred at the stage of elongation. By using the method of RNA-seq and q-RT-PCR analyses, we found that the spermatogenesis defects induced by *BmMael* mutation is associated with the tight-junction formation process and apoptosis.

2. Materials and methods

2.1. Silkworm strains

The multivoltine, nondiapausing silkworm strain, Nistari, was used for all experiments in this study. The larvae were reared on fresh mulberry leaves under standard conditions.

2.2. Plasmid construction

To establish the binary transgenic CRISPR/Cas9 system, two plasmids were constructed. The activator plasmid, *pBac [IE1-EGFP-nos-Cas9]*, was constructed to active the expression of Cas9 nuclease under the control of the *B. mori nanos* (*nos*) promoter. In the same plasmid, *EGFP* expression was driven by the *IE1* promoter. To construct the sequence-specific effector plasmid, *pBac [IE1-DsRed2-U6-sgRNA]*, the plasmid *pBac [IE1-DsRed2]* was used as the initial plasmid. The first U6 promoter (U6-1) sequences were PCR-amplified from silkworm genomic DNA using the primers HindIII-F and sg1-R. The primers sg1-F and Overlap-R were annealed to generate *BmMael* sgRNA1. The other U6 promoter (U6-2) sequence was PCR-amplified from the first U6 promoter using the primers Overlap-F and sg2-R. Similarly, sg2-F and HindIII-R were annealed to generate *BmMael* sgRNA2. Overlap extension PCR was performed with U6 and sgRNA to generate U6-sgRNA units. Subsequently, two U6-sgRNA units were cloned into *pBac [IE1-DsRed2]* using the ClonExpress MultiS One Step Cloning Kit (Vazyme). The primers used for plasmid construction are listed in Table S1 of the Supplementary Material.

2.3. Silkworm germline transformation

The mixture of transformation plasmids and helper plasmids were microinjected into preblastoderm G0 embryos, which were incubated at 25 °C in a humidified chamber for 10–12 days until larvae hatched. The G0 larvae were reared to moths and mated to wild-type (WT) moths. G1 progeny were scored for the presence of the fluorescent marker by observation under a Nikon AZ100 fluorescence microscope. The two transgenic lines were crossed to yield *BmMael* mutant heterozygous F1 progeny that were used in subsequent experiments.

2.4. Mutagenesis analysis

Genomic DNA was extracted from the heterozygotes using standard SDS lysis-phenol treatment, incubated with proteinase K, treated with RNase treatment, and purified. To perform gene-specific PCR amplification, 100 ng of the genomic DNA was used as template, and the primer pair, *Mael-seq-F* and *Mael-seq-R*, which flank both targets was used. The PCR products were extracted and cloned into the pJET-1.2 vector (Fermentas) and sequenced. The primers are listed in Table S1 of the Supplementary Material.

2.5. RNA isolation and cDNA synthesis

Total RNA was isolated from the gonads of three individual mutants and WT animals at the wandering stage using the TRIzol reagent (Invitrogen) according to the manufacturer's instructions, followed by treatment with DNase I (Invitrogen) and purification. An aliquot of 1 μg of the total RNA was used to synthesize cDNA using ReverAid First Strand cDNA Synthesis Kit (Fermentas). For piRNA detecting, the total RNA was firstly incubated with piRNA specific stem-loop primer at 65 °C for 5min, followed by normal cDNA synthesis steps according to the manufacturer's instructions.

2.6. Quantitative real-time PCR (qRT-PCR)

qRT-PCR analyses were performed using SYBR Green Real-time PCR Master Mix (Thermo Fisher Scientific) to analyze mRNA levels of selected genes and piRNA levels. PCR conditions were as follows: initial incubation of 95 °C for 5 min, followed by 40 cycles of 95 °C for 15 s and 60 °C for 1 min mRNA levels were normalized to levels of *B. mori ribosomal protein 49* (*Bmrp49*). The relative expression levels of piRNAs were measured using the stem-loop method, and the small RNA U6 was used as the internal reference. Three independent biological replicates of each qRT-PCR analysis were performed.

2.7. Immunoblot analysis

Proteins were extracted from the gonads when animals reached the wandering stage. Samples were homogenized and dissolved in PBS buffer. The concentration of total protein was measured by BCA Protein Assay Kit (Thermo), and 30 μg of extracted protein were separated by 12.5% SDS/PAGE and transferred to a PVDF membrane. The polyclonal rabbit anti-BmMAEL primary antibody recognizes the amino acids 87–409 of BmMAEL was used for BmMAEL detection (1:5000 dilution; Youke), and β-actin was detected using the mouse anti-β-actin primary antibody (1:5000 dilution; Vazyme Biotech) as the control. The specificity of anti-MAEL antibody was shown in Fig. S4B. For the secondary antibody, horseradish peroxidase-conjugated goat anti-rabbit and anti-mouse IgG (1:5000 dilution; Vazyme Biotech) were used. The ECL Plus Western blotting Detection Kit (GE Healthcare) was used to detect the protein signal.

2.8. Paraffin sectioning and hematoxylin-eosin staining

Testes of mutant and WT animals were dissected from the wandering stage larvae and prefixed with Qurnah's fixative (anhydrous ethanol: acetic acid: chloroform, 6:1:3 (v/v/v)). Samples were dehydrated three times using anhydrous ethanol, followed by clearing three times using xylene. Tissues were embedded in paraffin overnight, and cross-sections (5 μm) were cut with a Leica RM2235 microtome and stained using a mixture of hematoxylin and eosin to visualize

morphology. The stained sections were photographed by using an Olympus BX51 microscope.

2.9. Fluorescent staining of sperm bundles

Testes of mutant and WT animals were dissected from different stages (fourth larval stage to adult stage). Next, the testes were avulsed and the contents were fixed (Beyotime) for 1 h. Samples were then washed three times using PBS, followed by staining with TRITC Phalloidin (YEASEN) for 1 h. Nuclei were stained with Hoechst (Beyotime) for 10 min at room temperature. Samples were washed three times with PBS, dropped onto a microslide, and immediately analyzed by fluorescence microscopy (Olympus, BX53).

2.10. Transmission electron microscopy

Testes were dissected from pupal and adult stage mutant and WT animals and fixed with 2.5% glutaraldehyde in 0.1 M phosphate buffer (pH 7.2) overnight at 4 °C. Samples were washed with phosphate buffer and postfixed with 1% osmium tetroxide in phosphate buffer for 2 h. After washing, samples were dehydrated with ethanol in a series of concentrations and then embedded in Embed812 resin. Samples were cut into ultrathin sections (60–90 nm) and stained with 2% uranyl acetate (pH 5.0), followed by 10 mM lead citrate (pH 12). The stained sections were viewed with a Hitachi H-7650 transmission electron microscope.

2.11. RNA-seq analysis

Total RNA was extracted from testes of wandering stage larvae. Samples from three WT animals were pooled, and samples from three *BmMael* mutant animals were pooled. Samples were treated with DNase I to avoid genomic DNA contamination, purified, and dissolved in UltraPure distilled water (Invitrogen). The integrity of total RNA was confirmed using agarose electrophoresis, and 20 μg of each sample was sequenced (BGI). The genes differentially expressed in WT animals and *BmMael* mutants were identified. KEGG pathway and GO analyses were applied to identify pathways and processes altered in the *BmMael* mutants.

2.12. TUNEL staining assay

The paraffin sections were dewaxed twice by using xylene, followed by hydrating through exposure to a gradually decreasing series of ethyl alcohol (100%, 90%, 70%, 0%). The sections were then stained using One Step TUNEL Apoptosis Assay Kit (Beyotime) according to the manufacturer's instructions. The stained section were immediately analyzed by fluorescence microscopy (Olympus, BX53).

3. Results

3.1. Construction of BmMael mutants using CRISPR/Cas9

Quantitative real-time PCR (qRT-PCR) analysis showed that the expression of *BmMael* was much higher in gonads than in other organs at the three evaluated stages (Fig. S1). To explore the biological function of *BmMael*, we used a binary transgenic CRISPR/Cas9 system to generate *BmMael* mutants as previously described (Zhang et al., 2017). *BmMael* contains 13 exons with 12 introns, and we identified two small guide RNA (sgRNA) target sites following the rule of GGN19GG in exon 6 and exon 7 (Fig. 1B). The system consisted of two transgenic silkworm lines, which express Cas9 and sequence-specific sgRNAs separately. The expression of Cas9 was controlled by a *B. mori nanos* promoter (Xu et al., 2017, 2019), and sgRNAs were expressed from the U6 promoter (Fig. 1A); the lines were marked by EGFP and DsRed, respectively. When the two silkworm lines were crossed, the offspring expressed both Cas9 and sgRNAs, and, consequently, a mutation was generated in the *BmMael* locus (95%) to yield *ΔBmMael* animals. Sequencing ensured success of somatic mutagenesis in the *BmMael* locus (Fig. 1C). To avoid off-target effects, we detected 10 potential off-target sites, and didn't find any mutation. The potential off-target sites we detected was shown in Table S2. Furthermore, we used qRT-PCR and Western blot to evaluate the efficiency of the mutagenesis. Expression of *BmMael* was significantly down-regulated at both mRNA and protein levels in gonads of wandering stage *ΔBmMael* animals compared to WT individuals (Fig. 1D and E), confirming that the desired *BmMael* mutant strain was obtained.

3.2. BmMael is not involved in the silkworm sex determination

In *Drosophila*, *Mael* is essential for piRNA function but not for biogenesis of piRNA, and elimination of *Mael* results in derepression of TE expression (Sienski et al., 2012). In the silkworm, the piRNA *Fem* participates in female sex determination, and deletion of *Piwi* results in partial sexual reversal. The alternative splicing of *Bmdsx* is the reporter for masculinization and feminization (Li et al., 2018). No significant change in the *Bmdsx* splicing pattern was detected in *BmMael* mutants, indicating that MAEL is not involved in silkworm sex determination (Fig. S2A). To determine whether MAEL participates in the piRNA pathway in silkworm, we analyzed the relative abundances of six known piRNAs and seven TEs in the ovaries of WT and mutant animals. The levels of piRNAs and TEs in ovaries were not significantly different from WT levels in the *BmMael* mutants (Fig. S2B and Fig. S2D). This suggests that *BmMael* is not necessary for piRNA pathway in the ovary of silkworm. Moreover, we did not observe an obvious phenotype in the development of ovaries in the *BmMael* mutants (Fig. S2C).

3.3. BmMael is essential for spermatogenesis

Further analysis demonstrated that *BmMael* mutation resulted in male sterility. Compared with WT, the testes of *ΔBmMael* animals were much smaller at the same stage (Fig. 2A), which is similar to the *ΔBmMael* phenotype in mouse (Soper et al., 2008). Hematoxylin and eosin staining of paraffin-embedded tissue sections showed fewer sperm bundles in the testis of *BmMael* mutants than in WT animals (Fig. 2B). All the male mutants shown normal mating behavior and crossed with virgin wild female for 4 h. The male sterility was confirmed as almost no progeny were obtained in crosses of *ΔBmMael* males with WT virgin females (Fig. 2C and D).

Defects in spermatogenesis are usually responsible for male sterility (Metzendorf and Lind, 2010; Gomes and Civetta, 2014; Lorès et al., 2014). To investigate whether *BmMael* is necessary for spermatogenesis, we analyzed sperm development by fluorescence staining. At the early larval stage (third day of fourth larval stage, L4D3), almost all sperm were at the stage of spermatocysts in both WT and mutant males, and no obvious abnormality was observed in the mutants (data not shown). On the first day of fifth larval stage (L5D0) in WT animals, the eupyrene sperm bundle started to appear and elongate, and nuclei began to concentrate in the head of the bundle; while this step was defective in the *BmMael* mutants (Fig. S3A). The apyrene sperm bundles were generated during the wandering stage, similarly, the nuclei of apyrene sperm bundles could not aggregate to the middle part normally (Fig. S3B). With the elongation of sperm bundles, defects became more apparent in the mutants. In the *BmMael* mutants sperm, nuclei were not concentrated in the round head of eupyrene sperm nor the middle part of apyrene sperm, and shapes of sperm bundles were abnormal (Fig. 3).

Ultra-microstructural analyses of sperm bundles showed that there were fewer spermatozoa in each bundle in the *BmMael* mutants than in WT (Fig. 4A). In contrast to the orderly matrix formed by spermatozoa in WT, the spermatozoa in the sperm bundles of mutants were disordered (Fig. 4B). At the adult stage, few normal sperm were observed in the testes of mutants (Fig. 5). These findings revealed that *BmMael* is

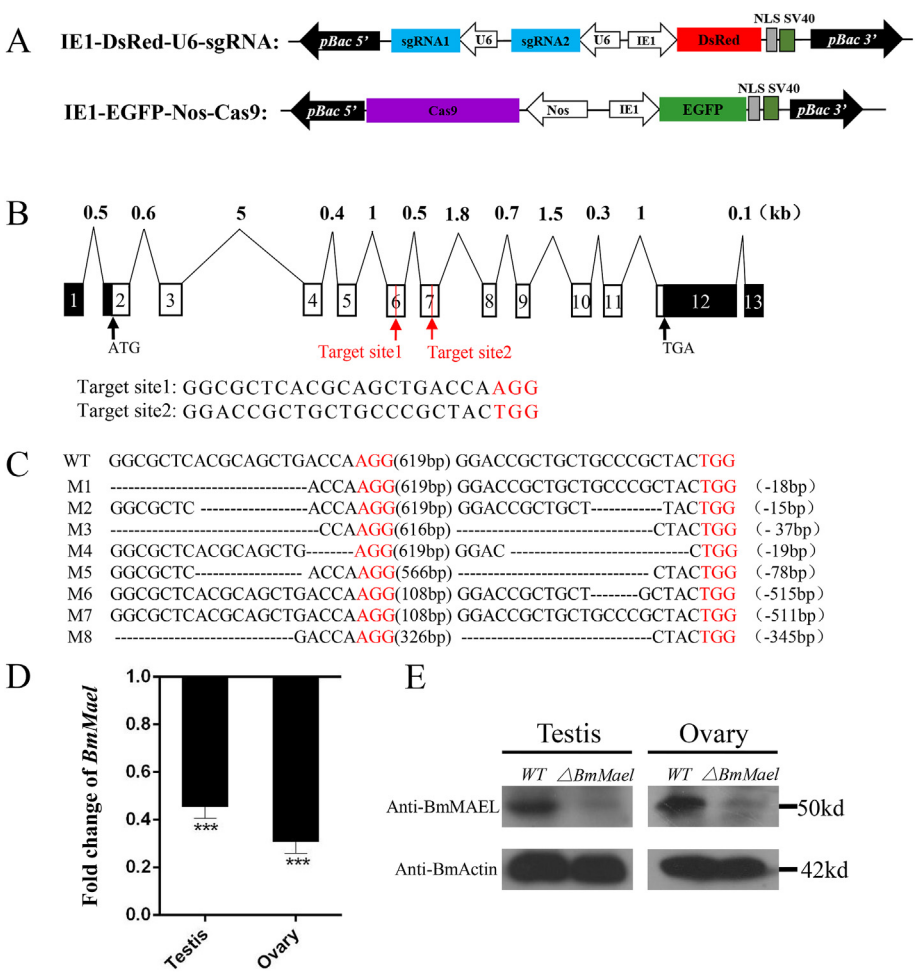

Fig. 1. Construction of *BmMael* mutants using the CRISPR/Cas9 system. (A) Schematic diagram of the *BmMael* gene structure and sgRNA-target sites. The boxes indicate the 13 exons of *BmMael* and lines represent the 12 introns. Lengths of each intron are indicated. The two sgRNA target sites located on the sense strand in exons 6 and 7 are marked with red lines. Start and stop codon locations are also indicated. (B) Plasmid construction for production of the transgenic silkworm. Expression of the *BmMael*-specific sgRNAs is driven by the U6 promoter and the expression of Cas9 is controlled by the *nanos* promoter. (C) Diverse types of mutations induced by CRISPR/Cas9 system. The wild-type (WT) sequence is shown at the top. The target sites are denoted in black, and the PAM sequence is in red. The dashed lines indicate deleted residues, and the deletion sizes are shown to the right of each sequence. (D) Q-RT-PCR analysis of *BmMael* mRNA expression in *ΔBmMael* relative to WT in testis and ovary at the wandering stage. Three individual biological replicates were performed, and error bars are ± SD. The asterisks (***) indicate significant differences relative to WT ($P < 0.001$, *t*-test). (E) Immunoblot analysis of *BmMael* protein expression level in gonads at the wandering stage. β-actin was used as control for equal loading. (For interpretation of the references to colour in this figure legend, the reader is referred to the Web version of this article.)

essential for spermatogenesis in the silkworm. Loss of MAEL resulted in defects during in elongation stage of spermatogenesis; specifically localization of nuclei was abnormal in *BmMael* mutants sperms.

3.4. Genes affected by the BmMael mutation

As *Mael* is a piRNA pathway gene in *Drosophila*, we analyzed the relative expression levels of several piRNAs and TEs in the testes of *BmMael* mutants. As was reported in *Drosophila* (Sienski et al., 2012), piRNA levels were not significantly different in *BmMael* mutant testes

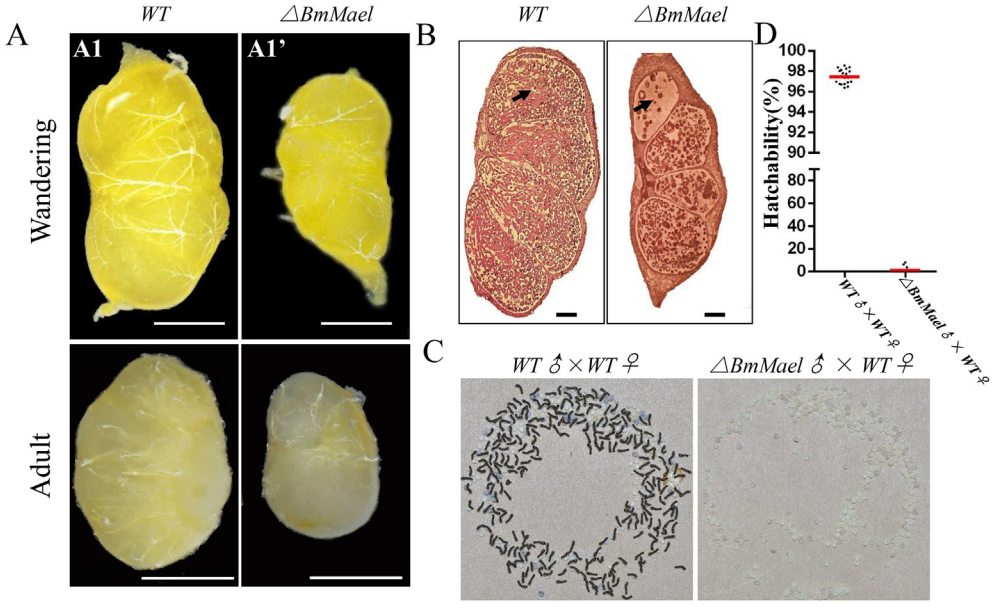

Fig. 2. Loss-of-function of *BmMael* leads to male sterility. (A) Representative images of testes of WT (left) and *ΔBmMael* (right) animals at the wandering stage (top row) and in adults (bottom row). Scale bar: 1 mm. (B) Representative images of the internal structures of the WT (left) and the *ΔBmMael* (right) testis at the wandering stage. Paraffin-embedded sections were stained with hematoxylin and eosin. Scale bar: 200 μm. Black arrows indicate sperm bundles. (C) Photograph of eggs from cross of WT male and WT female (left) and from cross of *ΔBmMael* male with WT female. (D) Percentage of oviposited eggs that hatched in crosses of 20 WT males and WT females and 20 *ΔBmMael* males with WT females.

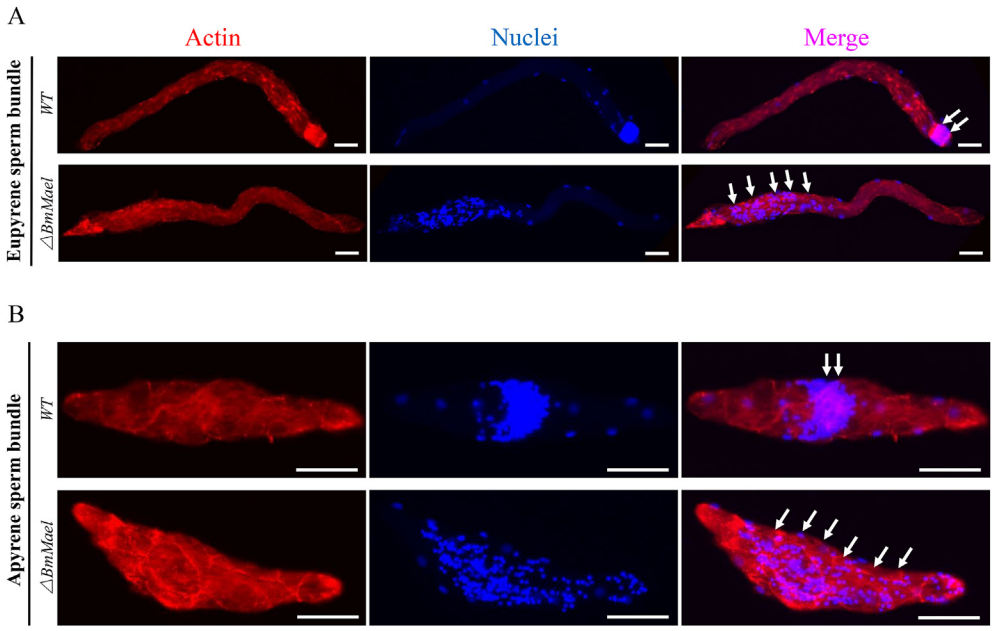

Fig. 3. *BmMael* mutation results in spermatogenesis defects. (A and B) Representative images of eupyrene sperm bundles (A) and apyrene sperm bundles (B) from WT (top) and *ΔBmMael* (bottom) on the first day of the pupal stage. The nuclei were stained with Hoechst 33258. TRITC-Phalloidin was used to stain actin to mark the outline of the sperm bundle. White arrows indicated nuclei. Scale bar, 50 μm.

compared to WT testes (Fig. 7A), however, expression of several TEs was significantly up-regulated (Fig. 7B). These results revealed a relative conserved function of *Maelstrom* in piRNA pathway.

To further explore the molecular mechanisms of the *ΔBmMael* spermatogenesis defects, RNA-seq analysis was performed using the mixed testes samples from three individual *ΔBmMael* animals and three individual WT animals at wandering stage. In total, we identified 4109 differentially-expressed genes (DEGs), among which 1003 genes were up-regulated and 3106 were down-regulated in *ΔBmMael* animals (Fig. S4A). According to GO functional classification, these genes were primarily involved in metabolic and cellular process and binding and catalytic activity (Fig. 6A). KEGG enrichment analysis showed that malaria, homologous recombination, apoptosis, pathogenic *Escherichia* coli infection, and tight junctions were the top five pathways (Fig. 6B).

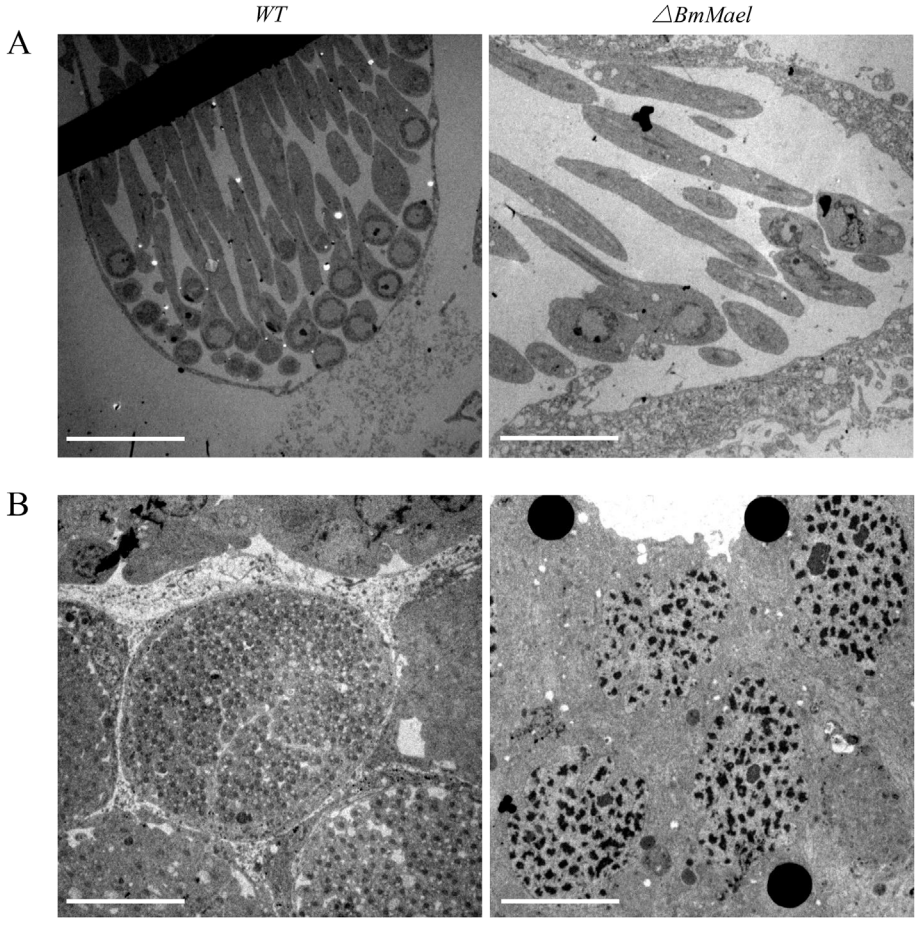

Fig. 4. Internal ultra-microstructures of sperm bundles visualized by transmission electron microscopy are abnormal in *BmMael* mutants. (A) Representative images of the internal structures of the eupyrene sperm bundles from WT (left) and *ΔBmMael* (right) animals on the first day of the pupal stage. Scale bar, 10 μm. (B) Representative images of the internal structures of the eupyrene sperm bundles from WT (left) and *ΔBmMael* (right) from adults. Cross section of a eupyrene sperm bundle. Scale bars, 10 μm.

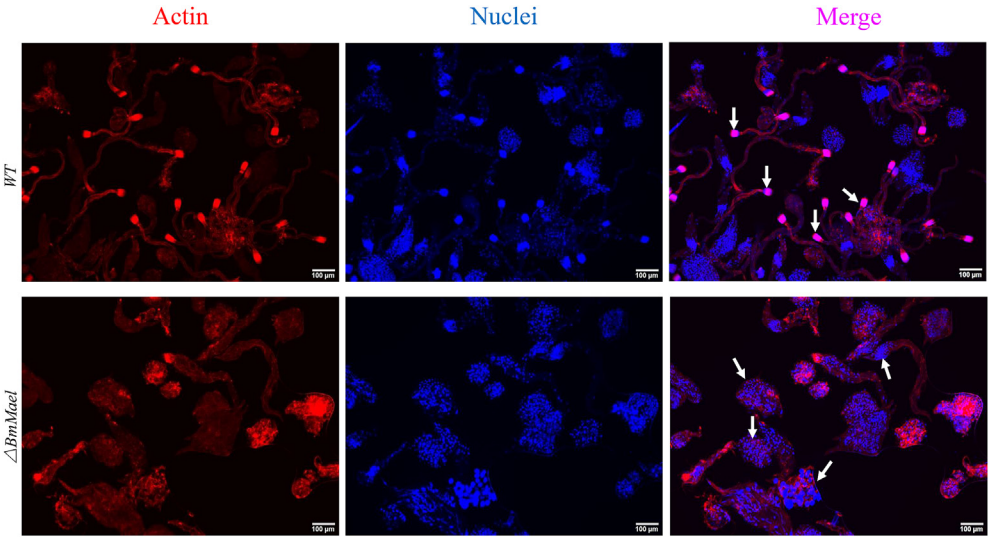

Fig. 5. Few normal sperm exist in the testes of adult *BmMael* mutants. Representative images of sperm bundles from adult WT (top) and *ΔBmMael* (bottom) animals. The nuclei were stained by Hoechst 33258. TRITC-Phalloidin was used to stain actin and marked the outline of the sperm bundle. White arrows indicated the nuclei. Scale bars, 100 μm.

As malaria and *E. coli* infection are related to human diseases, these are unlikely to be responsible for the phenotype observed. The shape abnormalities and disordered states in sperm bundles make it likely that tight junction and apoptosis pathway gene might play roles in the spermatogenesis defects.

Intercellular tight junctions hold cells together in vertebrates. Two barriers are involved: One is the paracellular barrier, which regulates selective paracellular permeability. The other is the intramembrane barrier, which serves as a 'fence' to restrict membrane component diffusion between the apical and basolateral membranes (Matter and Balda, 2003; Niessen, 2007; Zihni et al., 2016). In invertebrates, the corresponding junction is sometimes known as a septate junction (Banerjee et al., 2006; Ganot et al., 2015; Hall and Ward, 2016). *cdc42*, which encodes a protein necessary for the function of tight junctions (Rojas et al., 2001; Elbediwy et al., 2012) was upregulated 2.4 fold. mRNA levels of four genes known to encode tight junction components *angiomotin* (*amot*), *maguk, CAP-GLY* and *tub-α* (Wells et al., 2006; Yi et al., 2011; Peris et al., 2006; Yano et al., 2013; Zhang et al., 2018) were reduced in the mutant to 81.5%, 70.9%, 45.5%, and 20.1%, respectively, of WT levels (Fig. 7C). In addition, three genes, *Bmcaspase-n*, *Bmcaspase-8*, and *BmICE-5* (Sun et al., 2010; Zhang et al., 2010), which encode proteins that promote apoptosis, were up-regulated 6.9 fold, 2.9 fold, and 4.8 fold, respectively (Fig. 7D). TUNEL staining also showed apoptosis was enhanced in the testis of mutant (Fig. S5). These results indicate that the disruption of *BmMael* induces spermatogenesis defects that are related to tight junctions and apoptosis.

4. Discussion

In the current study, we used a binary transgenic CRISPR/Cas9 system to perform functional analysis of *BmMael*. In *B. mori*, the piRNA produced from the piRNA precursor *Fem* was necessary for sex determination, and deletion of the piRNA pathway gene *Piwi* resulted in partial sexual reversal (Kiuchi et al., 2014; Li et al., 2018). Despite its role in the piRNA pathway, our data indicated that MAEL is not involved in sex determination in the silkworm. Similarly, the piRNA factor Ago3 did not play a role in sex determination in the silkworm (Li et al., 2018). Our data showed that *BmMael* is essential for spermatogenesis as it was in *Drosophila* and mouse (Soper et al., 2008), revealing a conserved function of *Maelstrom*, all though the mechanisms of spermatogenesis were not the same in the three organisms. In *Drosophila*, MAEL ensures proper germline stem cell lineage differentiation by repressing microRNA-7. In mouse, MAEL is necessary for normal chromosome synapsis during meiosis (Soper et al., 2008; Pek et al., 2009). Our data indicated that the *BmMael* mutation in the silkworm induced spermatogenesis defects associated with tight junction formation, though the exact mechanism remains to be proven by more direct evidences.

In *Drosophila, Mael* was required for piRNA-induced TE silencing, and deletion of *Mael* resulted in TE derepression without affecting piRNA biogenesis (Sienski et al., 2012). Our results suggested that *BmMael* might not be essential for piRNA pathway in the ovary. However, our data showed that expression of several TEs was significantly up-regulated, thus, we speculated *BmMael* is essential for TEs silencing, though more data are needed to prove *BmMael* is involved in piRNA pathway. Actually, we were not sure whether the defects in spermatogenesis caused by the *BmMael* mutation were associated with TEs derepression, nevertheless, RNA-seq and qRT-PCR analyses demonstrated that spermatogenesis defects were associated with tight junctions and apoptosis. We hypothesize that the *BmMael* mutation results in derepression of TEs in testes of mutants, which in turn disrupt the expression of tight junction related genes by affecting genome stability. Consequently, the formation of the tight junction barrier between somatic support cells in sperm bundles was blocked, and sperm bundles did not form correctly. Due to failure of spermatogenesis, apoptosis was enhanced in testis. Though more data are needed to prove our hypothesis in silkworm, studies of *Drosophila* might provide an evidence from another side. In flies, a somatic permeability barrier formed by tight junctions around the germline cells is essential for spermatogenesis (Fairchild et al., 2015).

The close cooperation of the soma and germline is essential for spermatogenesis (França et al., 2012; Fairchild et al., 2015). In vertebrates, the blood-testes barrier (BTB) is the bridge between soma and germline. The BTB is formed by somatic Sertoli cells (Dym and Fawcett, 1970; Lui et al., 2003; Fairchild et al., 2015). If the BTB does not function correctly, spermatogenesis defects result that lead to male sterility (Gow et al., 1999; Mazaud-Guittot et al., 2010; Mok et al., 2012). Tight junctions are a component of the BTB; these structures restrict the movement of small molecules (Lui et al., 2003; Cheng and Mruk, 2012; Fairchild et al., 2015). In *Drosophila,* a somatic permeability barrier around the germline plays an analogous role to the BTB of vertebrates. Interestingly, septate junctions, which performed the same functions in invertebrate as tight junctions in vertebrates (Banerjee et al., 2006; Ganot et al., 2015; Hall and Ward, 2016), are also thought to be a part of the permeability barrier. Depletion of septate junction components results in failure of spermatogenesis (Fairchild et al., 2015). Our study indicates that septate junctions also appear to be essential for spermatogenesis in *B. mori*, though more direct evidences were needed.

This study describes the first functional analysis of *Mael* gene in

A

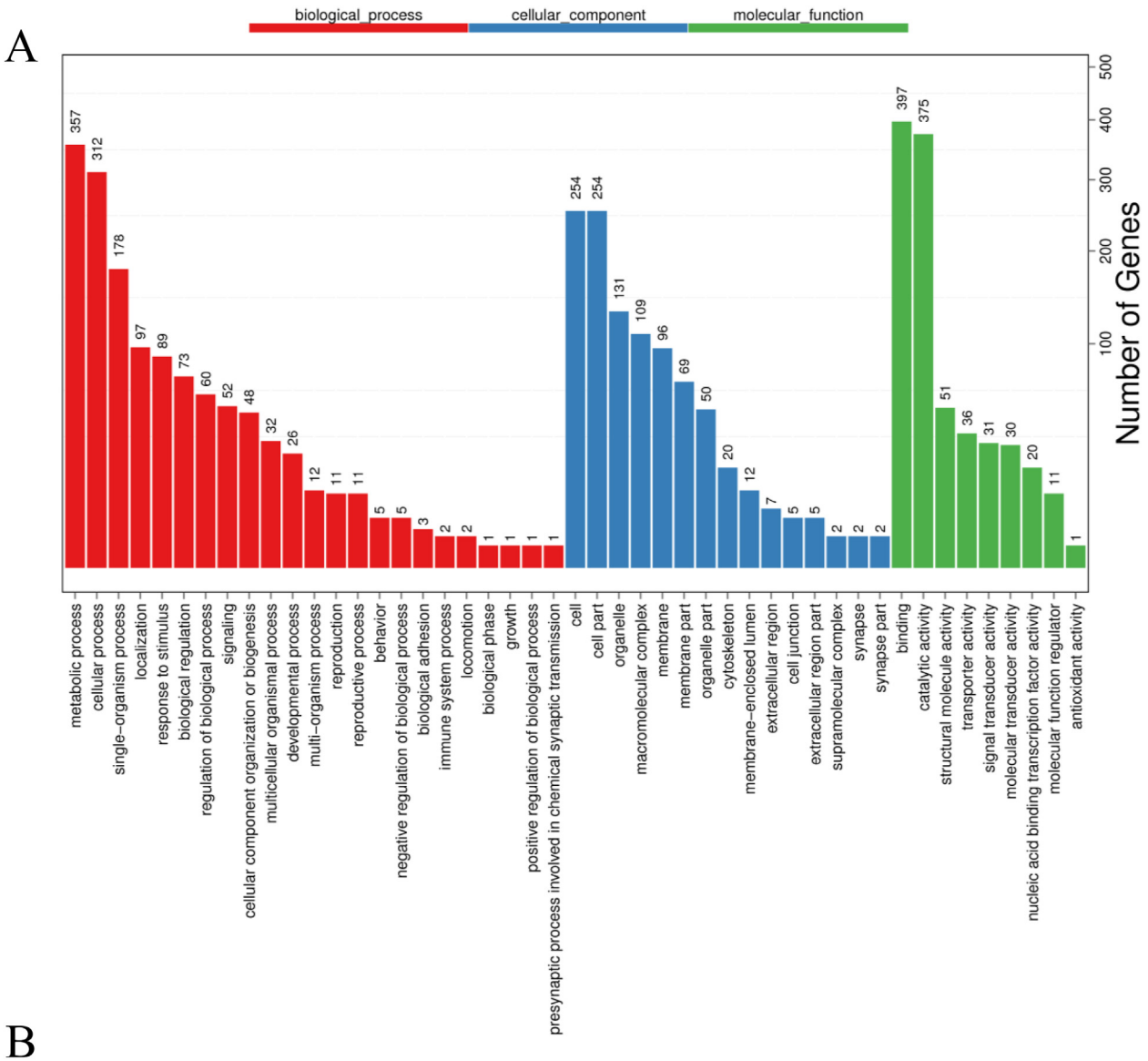

B

Pathway	Pathway ID	P-value
Malaria	ko05144	0.000354447
Homologous recombination	ko03440	0.000395903
Apoptosis	ko04210	0.001347117
Pathogenic Escherichia coli infection	ko05130	0.007076743
Tight junction	ko04530	0.007714452

Fig. 6. RNA-seq analysis showed altered gene expression in Δ*BmMael* animals. (A) The significantly enriched gene ontology terms for biological processes, cellular components, and molecular functions of the genes differentially expressed in *BmMael* mutants compared to WT. (B) The top five enriched KEGG pathways.

lepidopteran insects. In the silkworm *B. mori*, *Mael* was not involved in sex determination, but was essential for spermatogenesis, suggesting a conserved function of MAEL across different species including *Drosophila* and mouse. Moreover, our results revealed that *BmMael* mutation induced spermatogenesis defects is associated with septate junctions, in agreement with the vital function of septate junctions previously described in *Drosophila* spermatogenesis. The male sterility induced by *BmMael* depletion might be applicable in lepidopteran pest control.

Acknowledgments

We thank Xiaoyan Gao, Jiqin Li, and Zhiping Zhang (Shanghai Institute of Plant Physiology and Ecology, Shanghai Institutes for Biological Sciences, Chinese Academy of Sciences) for their help with transmission electron microscopy.

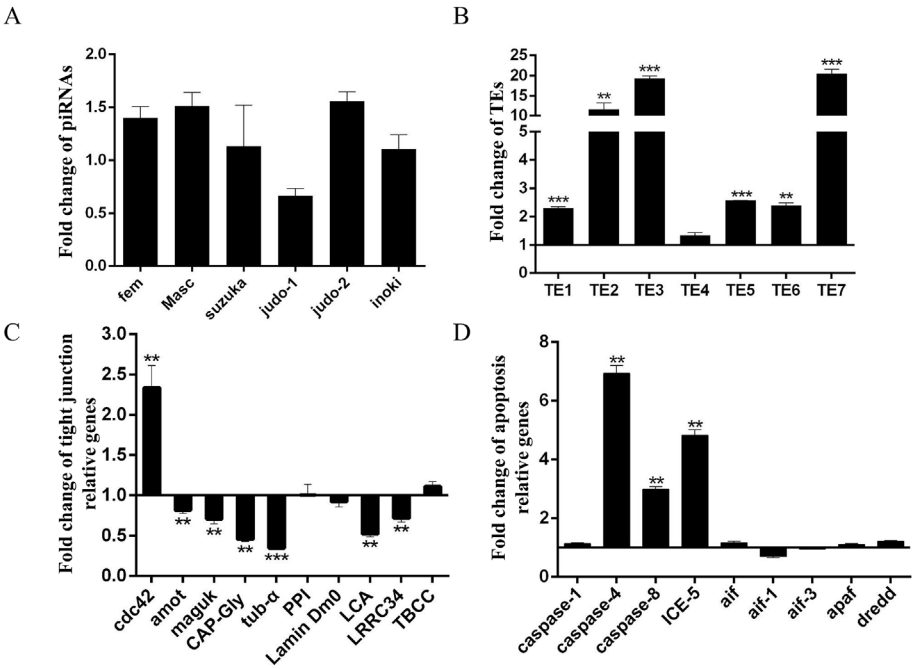

Fig. 7. TEs repression, apoptosis, and tight junction pathways are dysregulated in Δ*BmMael* animals. Fold changes in expression of selected A) piRNAs, B) TEs, C) genes encoding tight junction proteins, and D) apoptosis-related genes in the testes of *BmMael* mutants compared to WT at the wandering stage. Three individual replicates were used for qRT-PCR. Error bars are ± SD. The asterisks (*), (**), and (***) represent significant differences at the $p < 0.05$, 0.01, 0.001 levels, respectively (*t*-test).

This research was funded by the Strategic Priority Research Program of the Chinese Academy of Sciences (XDB11010600), the National Science Foundation of China (31420103918 and 31530072), and National Basic Research Program of China (2015CB755703).

Appendix A. Supplementary data

Supplementary data to this article can be found online at https://doi.org/10.1016/j.ibmb.2019.03.012.

References

Agarwal, A., Said, T.M., 2003. Role of sperm chromatin abnormalities and DNA damage in male infertility. Hum. Reprod. Update 9, 331–345.
Banerjee, S., Sousa, A.D., Bhat, M.A., 2006. Organization and function of septate junctions an evolutionary perspective. Cell Biochem. Biophys. 46, 65–77.
Chen, K.M., Campbell, E., Pandey, R.R., Yang, Z., McCarthy, A.A., Pillai, R.S., 2015. Metazoan Maelstrom is an RNA-binding protein that has evolved from an ancient nuclease active in protists. RNA 21, 833–839.
Cheng, C.Y., Mruk, D.D., 2012. The blood-testis barrier and its implications for male contraception. Pharmacol. Rev. 64, 16–64.
Clegg, N.J., Frost, D.M., Larkin, M.K., Subrahmanyan, L., Bryant, Z., Ruohola-Baker, H., 1997. Maelstrom is required for an early step in the establishment of *Drosophila* oocyte polarity: posterior localization of grk mRNA. Development 124, 4661–4671.
Cook, P.A., Wedell, N., 1999. Non-fertile sperm delay female remating. Nature 397, 486 486.
Czech, B., Hannon, G.J., 2016. One loop to rule them all: the ping-pong cycle and pirna-guided silencing. Trends Biochem. Sci. 41, 324–337.
Dym, M., Fawcett, D.W., 1970. The blood-testis barrier in the rat and the physiological compartmentation of the seminiferous epithelium. Biol. Reprod. 3, 308–326.
Elbediwy, A., Zihni, C., Terry, S.J., Clark, P., Matter, K., Balda, M.S., 2012. Epithelial junction formation requires confinement of Cdc42 activity by a novel SH3BP1 complex. J. Cell Biol. 198, 677–693.
Fairchild, M.J., Islam, F., Tanentzapf, G., 2017. Identification of genetic networks that act in the somatic cells of the testis to mediate the developmental program of spermatogenesis. PLoS Genet. 13, e1007026.
Fairchild, M.J., Smendziuk, C.M., Tanentzapf, G., 2015. A somatic permeability barrier around the germline is essential for *Drosophila* spermatogenesis. Development 142, 268–281.
França, L.R., Auharek, S.A., Hess, R.A., Dufour, J.M., Hinton, B.T., 2012. Blood-tissue barriers: morphofunctional and immunological aspects of the blood-testis and blood-epididymal barriers. Adv. Exp. Med. Biol. 763, 237–259.
Ganot, P., Zoccola, D., Tambutté, E., Voolstra, C.R., Aranda, M., Allemand, D., Tambutté, S., 2015. Structural molecular components of septate junctions in Cnidarians point to the origin of epithelial junctions in eukaryotes. Mol. Biol. Evol. 32, 44–62.
Gomes, S., Civetta, A., 2014. Misregulation of spermatogenesis genes in *Drosophila* hybrids is lineage-specific and driven by the combined effects of sterility and fast male regulatory divergence. J. Evol. Biol. 27, 1775–1783.
Gow, A., Southwood, C.M., Li, J.S., Pariali, M., Riordan, G.P., Brodie, S.E., Danias, J., Bronstein, J.M., Kachar, B., Lazzarini, R.A., 1999. CNS myelin and Sertoli cell tight junction strands are absent in osp/claudin-11 null mice. Cell 99, 649–659.
Hall, S., Ward, R.E., 2016. Septate junction proteins play essential roles in morphogenesis throughout embryonic development in *Drosophila*. G3 (Bethesda) 6, 2375–2384.
Kanippayoor, R.L., Alpern, J.H.M., Amanda, J., 2013. Moehring Protamines and spermatogenesis in *Drosophila* and Homo sapiens A comparative analysis. Spermatogenesis 3, 1–7.
Kawamura, N., Yamashiki, N., Bando, H., 1998. Behavior of mitochondria during eupyrene and apyrene spermatogenesis in the silkworm, *Bombyx mori* (Lepidoptera), investigated by fluorescence in situ hybridization and electron microscopy. Protoplasma 202, 223–231.
Kiuchi, T., Koga, H., Kawamoto, M., Shoji, K., Sakai, H., Arai, Y., Ishihara, G., Kawaoka, S., Sugano, S., Shimada, T., Suzuki, Y., Suzuki, M.G., Katsuma, S., 2014. A single female-specific piRNA is the primary determiner of sex in the silkworm. Nature 509, 633–636.
Li, Z., You, L., Yan, D., James, A.A., Huang, Y., Tan, A., 2018. *Bombyx mori* histone methyltransferase BmAsh2 is essential for silkworm piRNA-mediated sex determination. PLoS Genet. 14, e1007245.
Lorès, P., Vernet, N., Kurosaki, T., Van, P.T., Huylebroeck, D., Hikida, M., Gacon, G., Touré, A., 2014. Deletion of MgcRacGAP in the male germ cells impairs spermatogenesis and causes male sterility in the mouse. Dev. Biol. 386, 419–429.
Lui, W.Y., Mruk, D., Lee, W.M., Cheng, C.Y., 2003. Sertoli cell tight junction dynamics: their regulation during spermatogenesis. Biol. Reprod. 68, 1087–1097.
Meves, F., 1902. Uber oligopyrene und apyrene Spermien und Über ihre Entstehung, nach Beobachtungen an Paludina and Pygaera. Arch. Mikrosk. Anat. 61, 1–84.
Martin, R.H., 2008. Meiotic errors in human oogenesis and spermatogenesis. Reprod. Biomed. Online 16, 523–531.
Matsumoto, N., Sato, K., Nishimasu, H., Namba, Y., Miyakubi, K., Dohmae, N., Ishitani, R., Siomi, H., Siomi, M.C., Nureki, O., 2015. Crystal structure and activity of the endoribonuclease domain of the piRNA pathway factor Maelstrom. Cell Rep. 11, 366–375.
Matter, K., Balda, M.S., 2003. Signalling to and from tight junctions. Nat. Rev. Mol. Cell Biol. 4, 225–236.
Matunis, E.L., Stine, R.R., Cuevas, M., 2012. Recent advances in *Drosophila* male germline stem cell biology. Spermatogenesis 2, 137–144.
Mazaud-Guittot, S., Meugnier, E., Pesenti, S., Wu, X., Vidal, H., Gow, A., Le, M.B.B., 2010. Claudin 11 deficiency in mice results in loss of the Sertoli cell epithelial phenotype in the testis. Biol. Reprod. 82, 202–213.
Metzendorf, C., Lind, M.I., 2010. *Drosophila* mitoferrin is essential for male fertility: evidence for a role of mitochondrial iron metabolism during spermatogenesis. BMC Dev. Biol. 10, 68 68.
Mok, K.W., Mruk, D.D., Lee, W.M., Cheng, C.Y., 2012. Spermatogonial stem cells alone are not sufficient to re-initiate spermatogenesis in the rat testis following adjudin-induced infertility. Int. J. Androl. 35, 86–101.
Niessen, C.M., 2007. Tight junctions/adherens junctions: basic structure and function. J. Investig. Dermatol. 127, 2525–2532.
Osanai, M., Kasuga, H., Aigaki, T., 1987. Physiological-role of apyrene spermatozoa of bombyx-mori. Experientia 43, 593–596.
Pek, J.W., Lim, A.K., Kai, T., 2009. *Drosophila* Maelstrom ensures proper germline stem cell lineage differentiation by repressing microrna-7. Dev. Cell 17, 417–424.
Peris, L., Thery, M., Fauré, J., Saoudi, Y., Lafanechère, L., Chilton, J.K., Gordon-Weeks, P., Galjart, N., Bornens, M., Wordeman, L., Wehland, J., Andrieux, A., Job, D., 2006.

Tubulin tyrosination is a major factor affecting the recruitment of CAP-Gly proteins at microtubule plus ends. J. Cell Biol. 174, 839–849.
Rettie, E.C., Dorus, S., 2012. *Drosophila* sperm proteome evolution Insights from comparative genomic approaches. Spermatogenesis 2, 213–223.
Riemann, J.G., George III, Gassner, 1973. Ultrastructure of Lepidopteran sperm within spermathecae. Ann. Entomol. Soc. Am. 66, 154–159.
Rojas, R., Ruiz, W.G., Leung, S.M., Jou, T.S., Apodaca, G., 2001. Cdc42-dependent modulation of tight junctions and membrane protein traffic in polarized Madin-Darby canine kidney cells. Mol. Biol. Cell 12, 2257–2274.
Sahara, K., Takemura, Y., 2003. Application of artificial insemination technique to eupyrene and/or apyrene sperm in *Bombyx mori*. J. Exp. Zool. A Comp. Exp. Biol. 297, 196–200.
Sato, K., Siomi, M.C., 2016. Functional and structural insights into the piRNA factor Maelstrom. FEBS Lett. 589, 1688–1693.
Siddall, N.A., Hime, G.R., 2017. *Drosophila* toolkit for defining gene function in spermatogenesis. Reproduction 153, R121–R132.
Sienski, G., Dönertas, D., Brennecke, J., 2012. Transcriptional silencing of transposons by piwi and Maelstrom and its impact on chromatin state and gene expression. Cell 151, 964–980.
Siomi, M.C., Sato, K., Pezic, D., Aravin, A.A., 2011. PIWI-interacting small RNAs: the vanguard of genome defence. Nat. Rev. Mol. Cell Biol. 12, 246–258.
Slotkin, R.K., Martienssen, R., 2007. Transposable elements and the epigenetic regulation of the genome. Nat. Rev. Genet. 8, 272–285.
Soper, S.F.C., Heijden, G.W.V.D., Hardiman, T.C., Goodheart, M., Martin, S.L., Boer, P.D., Bortvin, A., 2008. Mouse Maelstrom, a component of nuage, is essential for spermatogenesis and transposon repression in meiosis. Dev. Cell 15, 285–297.
Sun, Y., Wang, W., Li, B., Wu, Y., Wu, H., Shen, W., 2010. Synchronized expression of two caspase family genes, *ice-2* and *ice-5*, in hydrogen peroxide-induced cells of the silkworm, *Bombyx mori*. J. Insect Sci. 10, 43 43.
Tóth, K.F., Pezic, D., Stuwe, E., Webster, A., 2016. The piRNA pathway guards the germline genome against transposable elements. Adv. Exp. Med. Biol. 886, 51–77.
Wells, C.D., Fawcett, J.P., Traweger, A., Yamanaka, Y., Goudreault, M., Elder, K., Kulkarni, S., Gish, G., Virag, C., Lim, C., Colwill, K., Starostine, A., Metalnikov, P., Pawson, T., 2006. A Rich1/Amot complex regulates the Cdc42 GTPase and apical-polarity proteins in epithelial cells. Cell 125, 535–548.
Xu, J., Chen, S., Zeng, B., James, A.A., Tan, A., Huang, Y., 2017. *Bombyx mori* P-element somatic inhibitor (BmPSI) is a key auxiliary factor for silkworm male sex determination. PLoS Genet. 13, e1006576.
Xu, J., Chen, R.M., Chen, S.Q., Chen, K., Tang, L.M., Yang, D.H., Yang, X., Zhang, Y., Song, H.S., Huang, Y.P., 2019. Identification of a germline-expression promoter for genome editing in *Bombyx mori*. Insect Sci. 00, 1–9.
Yamashiki, N., Kawamura, N., 2003. Behaviors of nucleus, basal bodies and microtubules during eupyrene and apyrene spermiogenesis in the silkworm, *Bombyx mori* (Lepidoptera). Dev. Growth Differ. 39, 715–722.
Yano, T., Matsui, T., Tamura, A., Uji, M., Tsukita, S., 2013. The association of microtubules with tight junctions is promoted by cingulin phosphorylation by AMPK. J. Cell Biol. 203, 605–614.
Yi, C., Troutman, S., Fera, D., Stemmer-Rachamimov, A., Avila, J.L., Christian, N., Persson, N.L., Shimono, A., Speicher, D.W., Marmorstein, R., Holmgren, L., Kissil, J.L., 2011. A tight junction-associated Merlin-angiomotin complex mediates Merlin's regulation of mitogenic signaling and tumor suppressive functions. Cancer Cell 19, 527–540.
Zhang, L., Feng, T., Spicer, L.J., 2018. The role of tight junction proteins in ovarian follicular development and ovarian cancer. Reproduction 155, 183–198.
Zhang, J.Y., Pan, M.H., Sun, Z.Y., Huang, S.J., Yu, Z.S., Liu, D., Zhao, D.H., Lu, C., 2010. The genomic underpinnings of apoptosis in the silkworm, *Bombyx mori*. BMC Genomics 11, 611 611.
Zhang, Z., Liu, X., Shiotsuki, T., Wang, Z., Xu, X., Huang, Y., Li, M., Li, K., Tan, A., 2017. Depletion of juvenile hormone esterase extends larval growth in *Bombyx mori*. Insect Biochem. Mol. Biol. 81, 72–79.
Zihni, C., Mills, C., Matter, K., Balda, M.S., 2016. Tight junctions: from simple barriers to multifunctional molecular gates. Nat. Rev. Mol. Cell Biol. 17, 564–580.